Mutant nucleophosmin and cooperating pathways drive leukemia initiation and progression in mice

Nat Genet. Author manuscript; available in PMC 2011 November 01.

Published in final edited form as:
Nat Genet. 2011 May ; 43(5): 470–475. doi:10.1038/ng.796.

Mutant nucleophosmin and cooperating pathways drive leukemia initiation and progression in mice

George S. Vassiliou[1,*], **Jonathan L. Cooper**[1], **Roland Rad**[1], **Juan Li**[2], **Stephen Rice**[1], **Anthony Uren**[3], **Lena Rad**[1], **Peter Ellis**[1], **Rob Andrews**[1], **Ruby Banerjee**[1], **Carolyn Grove**[1], **Wei Wang**[1], **Pentao Liu**[1], **Penny Wright**[4], **Mark Arends**[4], and **Allan Bradley**[1,*]

[1]Mouse Genomics Team, The Wellcome Trust Sanger Institute, Wellcome Trust Genome Campus, Hinxton, Cambridge, CB10 1SL, United Kingdom. [2]Department of Haematology, Cambridge Institute for Medical Research, University of Cambridge, Hills Road, Cambridge, United Kingdom. [3]The Netherlands Cancer Institute, Plesmanlaan 121, 1066 CX Amsterdam, The Netherlands. [4]Department of Pathology, University of Cambridge, Addenbrooke's Hospital, Hills Road, Cambridge, CB2 2QQ, United Kingdom.

Abstract

Acute myeloid leukemia (AML) is a molecularly diverse malignancy with a poor prognosis, whose largest subgroup is characterized by somatic mutations in *NPM1*, the gene for Nucleophosmin[1]. These mutations, termed *NPM1c*, result in cytoplasmic dislocation of Nucleophosmin[1] and are associated with distinctive transcriptional signatures[2], yet their role in leukemogenesis remains obscure. Here we report that activation of a humanized *Npm1c* knock-in allele in murine hemopoietic stem cells causes *Hox* overexpression, enhanced self-renewal and expanded myelopoiesis. One third of mice developed delayed-onset AML, suggesting a requirement for cooperating mutations. We identified such mutations using a *Sleeping Beauty*[3,4] transposon which caused rapid-onset AML in 80% of *Npm1c*+ mice, associated with mutually exclusive integrations in *Csf2*, *Flt3* or *Rasgrp1* in 55 of 70 leukemias. Recurrent integrations were also identified in known and novel leukemia genes including *Nf1, Bach2, Dleu2 and Nup98*. Our results give new pathogenetic insights and identify therapeutic targets in NPM1c+ AML.

Nucleophosmin, has roles in several cellular processes including ribosome biogenesis and centrosome duplication[5,6], for which it relies on its ability to shuttle between the nucleolus, nucleus and cytoplasm using subcellular localization signals[7]. This ability is impaired in 35% of AMLs, as a result of *NPM1c* mutations[1] which disrupt the N-terminal nucleolar localization signal of Nucleophosmin and generate a nuclear export signal in its place[1,8].

[*]Corresponding authors. Correspondence and requests for materials should be addressed to A.B. (a.bradley@sanger.ac.uk) or G.V. (gsv20@sanger.ac.uk)..

Database Accession numbers: Microarray data and description of experimental design were deposited to Array Express with accession number E-MEXP-3113.

Author Contributions. G.V. and A.B. designed the study; G.V. generated *Npm1*$^{flox\text{-}cA}$ mice, *GrOnc* mice and GFP-NPM1 constructs, managed mouse colonies, designed and validated polyclonal anti-Npm1c sera and carried out western blots; J.L.C. and G.V. performed mouse genotyping, tumor processing/banking and K562 transfections; G.V., J.C., R.R. and L.R. performed mouse necropsies; G.V. J.L.C. and J.C. performed hemopoietic analyses; G.V. and C.G. performed qPCR; G.V., P.E. and R.A. performed gene expression analysis studies; S.R, G.V. and R.R. performed mapping and analysis of transposon integration sites; G.V. and R.B. performed fluorescence-in-situ hybridization; W.W. and P.L. generated the *Stella-Cre* mice; A.U. generated the *Rosa*$^{flox\text{-}SB}$ mice; P.W. and M.A. performed histological analyses; A.B. supervised the study; all authors contributed to the writing of the manuscript.

The authors have no competing financial interests to declare

Europe PMC Funders Author Manuscripts

NPM1c mutations are mutually exclusive of fusion genes found in other types of AML[9], but frequently co-occur with activating mutations in *FLT3*[1] or *RAS*[10].

NPM1c is known to bind to and alter the subcellular distribution of several proteins including *HEXIM1*, *Fbw7γ*, *p19Arf* and *NF-kappaB*[8], however the relevance of these interactions to AML is unknown[8]. Selected transgenic mouse lines overexpressing *NPM1c* in myeloid progenitors display an increased incidence of mild myeloproliferative syndromes, but the significance of this observation is unclear as these mice do not develop AML[11].

To study the hemopoietic effects of *NPM1c*, we generated a conditional knock-in mouse model of the commonest form of *NPM1c* mutation, type A[1]. We confirmed that the human (NPM1^{cA}) and "humanized" mouse (Npm1^{cA}) type A mutant proteins (Supplementary figure 1) displayed the same sub-cellular localization (Figure 1a) and proceeded to modify the *Npm1* locus in mouse embryonic stem (ES) cells. The conditional allele, *Npm1$^{flox\text{-}cA}$*, was designed to minimize interference with the native locus, as this could itself be leukemogenic[12], yet switch to the mutant allele, *Npm1^{cA}*, after Cre-*loxP* recombination (Figure 1b). We confirmed that after Cre-*loxP* recombination *Npm1$^{flox\text{-}cA/+}$* ES cells expressed the Npm1^{cA} mutant mRNA and protein (Figure 1c,d), and established the *Npm1$^{flox\text{-}cA/+}$* allele in mice which were born at Mendelian ratios. However, the *Npm1^{cA}* allele was incompatible with normal embryonic development as crosses between *Npm1$^{flox\text{-}cA/flox\text{-}cA}$* mice and mice heterozygous for *Stella-Cre*, which mediates Cre-*loxP* recombination in the early embryo (PL, unpublished), gave no double transgenic live offspring (0/80) or embryos at E8 (n=11), E10 (n=10) and E12 (n=23). By contrast, the offspring of *Npm1$^{flox\text{-}cA/flox\text{-}cA}$* – *Mx1-Cre^{+}* crosses were born at Mendelian ratios (Figure 1e).

To study the hemopoietic effects of *Npm1^{cA}*, 5- to 8-week-old *Npm1$^{+/+}$* and *Npm1$^{flox\text{-}cA/+}$* mice (hereafter collectively referred to as *Npm1^{WT}*) and *Npm1$^{flox\text{-}cA/+}$; Mx1-Cre^{+}* mice (hereafter referred to as *Npm1$^{cA/+}$*), were treated with Polyinosinic-Polycytidylic acid (pIpC) and analyzed 8 weeks later. Cre-*lox*P recombination was seen in >90% of bone-marrow-derived hemopoietic colonies from *Npm1$^{cA/+}$* mice (Supplementary Figure 2), reflecting efficient recombination in hemopoietic stem cells (HSCs) and Npm1^{cA} protein was detectable in *Npm1$^{cA/+}$* hemopoietic tissues (Figure 2a). Gene expression profiling of *Npm1$^{cA/+}$* compared to *Npm1^{WT}* lineage negative marrow progenitors (Lin^{-}), showed differential overexpression of *HoxA5*, *HoxA7*, *HoxA9*, *HoxA10* and *HoxB5* genes (Figure 2b and Supplementary Table 1). Similar gene expression changes were seen with total bone marrow nucleated cells (BMNC) and B220+ cells, but not Gr1+/Mac1+ cells (Supplementary tables 2-4). For *Npm1$^{cA/+}$* BMNC *HoxA9*, *HoxA7* and *HoxA5* were the 3 most significantly overexpressed mRNAs in the mouse genome and expression of several lymphoid-specific genes was reduced (Supplementary table 2). Total *Npm1* mRNA expression was unaltered (Supplementary tables 1-4 and Supplementary figure 3).

Npm1$^{cA/+}$ and *Npm1^{WT}* blood counts did not differ (Figure 2c); although *Npm1$^{cA/+}$* mice had increased mean red cell (MCV) and platelet (MPV) volumes (Figure 2d). Bone marrow histo-morphological examination revealed no detectable abnormalities/differences (Supplementary Figure 4a). Flow cytometric analysis of marrow cells showed no significant differences in stem or progenitor cell compartment sizes (Figure 2e-f and Supplementary Figure 4b). However, *Npm1$^{cA/+}$* mice had increased numbers of Gr1+/Mac1+ myeloid cells and decreased numbers of late B-cells (B220+/CD19+) (Figure 2g-i). Additionally, Npm1$^{cA/+}$ cells showed increased serial re-plating ability in methylcellulose, an in vitro surrogate for self-renewing potential[13] (Figure 2j). There were no differences in levels of Gr1+/Mac1+ cell apoptosis or DNA damage (Supplementary Figure 4c-e).

To study the leukemogenicity of Npm1^{cA}, we aged 43 *Npm1*$^{cA/+}$ and *44 Npm1*^{WT} mice. *Npm1*$^{cA/+}$ mice had a shorter overall survival compared to *Npm1*^{WT} animals (617 vs 769 days, p=0.018) as a result of excess deaths due to AML (13 vs 0, p=0.0001) (Figure 2k-l). Morphologically AMLs showed maturation ("myeloid leukemia with maturation"[14]) and all 5 AMLs tested were Gr1+/Mac1+. Of 13 *Npm1*$^{cA/+}$ mice with AML, 6 were found to have coincidental non-extensive B-lymphoid tumors. Compared to Npm1$^{cA/+}$ mice dying of non-hematological causes, mice with AML had enlarged livers (2.6g vs 1.8g, p<0.001) and spleens (1.3g vs 0.3g, p<0.001) and higher blood leukocyte counts (77.1 vs 7.0 $\times 10^6$/l, p=0.006)(Supplementary table 5). Also 2/2 AMLs tested were transplantable into sublethally irradiated syngeneic mice (Supplementary table 6). Finally, *Npm1*$^{cA/+}$ and *Npm1*^{WT} mice developed lymphoid tumors at the expected rate for their age/strain[15] and had similar rates of non-hematological mortality (Figure 2k and Supplementary table 5).

The above data show that Npm1c can initiate AML, however the long latency reflects the need for additional mutations. To identify cooperating mutations, we subjected *Npm1*$^{cA/+}$ mice to insertional mutagenesis with *Sleeping Beauty* (SB)[3]. We generated transgenic mice carrying approximately 80 copies of *GrOnc*, a novel bi-functional *PiggyBac/SB transposon*[16] capable of both gene activation and disruption (Figure 3a-b and Supplementary Figure 5). *GrOnc* harbors the Graffi1.4 murine leukemia virus LTR, which preferential promotes myeloid rather than lymphoid leukemia in predisposed backgrounds, an effect attributed to the LTR[17].

We crossed *Npm1*$^{flox\text{-}cA/+}$, *GrOnc*, *Mx1-Cre* and conditional *Rosa26*$^{flox\text{-}SB}$ transposase (Supplementary Figure 6) mouse lines as per Supplementary Figure 7a to generate 125 *Npm1*$^{flox\text{-}cA/+}$*; Rosa*$^{flox\text{-}SB/+}$*; GrOnc*$^{+}$*; Mx1-Cre*$^{+}$ (*Npm1*$^{cA/+}$ mutagenesis cohort), and 45 *Npm1*$^{+/+}$*; Rosa*$^{flox\text{-}SB/+}$*; GrOnc*$^{+}$*; Mx1-Cre*$^{+}$ (*Npm1*$^{+/+}$ mutagenesis cohort). All mutagenised mice developed aggressive leukemia/lymphoma within one year of pIpC induction (Figure 3c). However, mean survival was significantly shorter in the *Npm1*$^{cA/+}$ compared to *Npm1*^{WT} mice (99 vs. 150 days, p=0.001) (Figure 3c). The first 121 mice (87 *Npm1*$^{cA/+}$ and 34 *Npm1*$^{+/+}$) were studied in detail and tumors classified by histological type (Supplementary Table 6), confirmed by flow cytometry in 18 leukemias. Compared to *Npm1*$^{+/+}$, *Npm1*$^{cA/+}$ mice had a significantly higher fraction of AMLs (80.5% vs. 26.5%, p=0.00000002) and no T-cell leukemias (0% vs. 17.6%, p=0.00006) (Figure 3d-f). These findings indicate strong synergy between *Npm1*^{cA} and *GrOnc* in promoting myeloid leukemogenesis. In some mice a coincidental second tumor was identified (leukemia/ lymphoma in 19.8% and angiosarcoma in 3.3%) (Supplementary Table 7).

In order to identify the genetic mutations collaborating with *Npm1c* to cause AML, we mapped the transposon integration sites in hemopoietic tumors from 87 *Npm1*$^{cA/+}$ and 34 *Npm1*$^{+/+}$ mice using barcoded splinkerette PCR and 454-sequencing. A total of 219,556 high-quality reads mapped evenly throughout the genome although, as expected for SB[3-4], we observed local hopping around the *GrOnc* donor site at Megabase (Mb) 30 on chromosome 19 (Supplementary Figure 8). CISs for *Npm1*$^{cA/+}$ and *Npm1*$^{+/+}$ tumors were identified using the kernel convolution method[18] and those mapping within 2Mb of the donor site discarded. The only other CIS on chromosome 19 involved *Pten* located at 32.8Mb, which makes its significance uncertain. The CIS sets in *Npm1*$^{cA/+}$ and *Npm1*$^{+/+}$ tumors included several known and many putative novel leukemia genes (Figure 4a, Supplementary Figures 8 and 9). The two sets overlapped but were clearly different, indicating that distinct molecular pathways operated in the two groups.

In the *Npm1*^{cA} group, the most striking finding was the identification of activating integrations upstream of *Csf2*, the gene for Gm-csf, in 48.3% of leukemias, associated with *LunSD-Csf2* fusion transcripts, Csf2 mRNA overexpression (Figure 4b-d) and increased

levels of Gm-csf in leukemic cell supernatants (p=0.0007, Supplementary Table 8). We studied transposon integrations in single-cell derived methylcellulose colonies from three *Csf2*+ AMLs and found that over 90% of CFU colonies (11/12, 12/12 and 19/20) carried *Csf2* insertions. We went on to map transposon integrations in 3 such colonies from the AML 36 and found that individual colonies carried 67-90 independent integrations each, yet only two integrations were shared between them, those involving *Csf2* and the myeloid oncogene *Myst4* (*Moz*) (Figure 4e). This is the first study of the subclonal make-up of transposon-derived malignancies and shows that, if the transposase remains active, transposons are continuously re-mobilized generating a highly heterogeneous population; bar for a small number of key insertions, possibly the leukemia "drivers". We went on to study transposon integrations in leukemias developing in irradiated recipients transplanted with AMLs 26 and 38. We found that *Csf2* insertions persisted in all 5 recipient mice studied (Supplementary Table 5), whilst the vast majority (>98%) of other insertions were lost. These data strongly indicate that *Csf2* insertions are critical to the growth of these leukemias and thus persist during leukemic evolution/propagation, whilst "passenger" insertions are lost. *Csf2* can behave as a myeloid oncogene in mice when activated by endogenous retroviruses[19], whilst autocrine Gm-csf production has been reported to drive the growth of human AML blasts in-vitro [20]-[21] and this is usually, albeit not always, inhibited by anti-GM-CSF antibodies.

Other important CISs included *Flt3* (Figure 4f), a gene frequently co-mutated in human NPM1c+ AML and *Nup98* (Figure 4g), a key component of the nuclear pore and a leukemogenic fusion gene partner not been previously identified as a retroviral or transposon CIS. NUP98 fusion proteins can directly interfere with nucleo-cytoplasmic transport of NPM1c[22], raising the possibility that *Nup98* insertions may operate in a similar way hence their specificity to $Npm1^{cA/+}$ AMLs. Other CISs included inactivating *GrOnc* insertions in signal transduction inhibitors such as *Nf1*, *Ptpn1* and *Ptptn2* and insertions in transcription factors including *Bach2*, *Cnot1, Pax5* and *Zfp521* (Figure 5a and Supplementary figure 10).

Co-occurrence analysis of CIS genes from $Npm1^{cA/+}$ AMLs, showed that Csf2 integrations were mutually exclusive of integrations in *Flt3* (p=0.002) and *Rasgrp1* (p=0.008) (Figure 5a and Supplementary figure 11). This was also true for *Kras* but did not reach statistical significance (p=0.12). These observations suggest that these genes provide alternative proliferation signals that complement Npm1c in promoting cellular transformation. Interestingly *Rasgrp1*, previously associated with T-lymphoblastic leukemia in retroviral mutagenesis screens[23], was recently identified as a drug resistance gene in another mouse model of AML[24]. *Hox* overexpression persisted in $Npm1^{c/+}$ transposon-derived AMLs, irrespective of transposon insertions, suggesting that the molecular effects of Npm1c mutations remained operative in leukemic cells (Figure 5b). *HoxA7* and *HoxA9* are frequently targeted by retroviruses in BXH2 myeloid leukemias[25] and mediate leukemic transformation by MLL oncoproteins[26]. Also, in line with our findings, $HoxA9^{-/-}$ mice exhibit defects in maturing myeloid and B-lymphoid cells, but not early progenitors[27]. Overall, this makes it highly plausible that *Hox* overexpression mediates the leukemogenic effects of NPM1c, particularly as expression levels seen in our mice are comparable to those in human AMLs.

Taken together, our data demonstrate that Npm1c are AML-initiating mutations which cause *Hox* overexpression, impart increased self-renewal to and prime hemopoietic stem/progenitor cells to leukemic transformation by activation of a narrow set of pro-proliferative molecules/pathways, usually in combination with mutations in transcriptional regulators (Figure 5c, Supplementary Tables 1-3). Observations from whole genome sequencing studies are generating data in support of such a model in this and other subgroups of AML

with a normal karyotype[10,28]. Also, our data explain other important features of human NPM1c+ AML, including a consistent negativity for the primitive marker CD34[1] (effects of Npm1^{cA} most noticeable on later progenitors) and a failure to observe NPM1c mutations in the human germline (embryonic lethality). Finally, our approach to define the effects of a mutation in isolation and proceed to map its collaborative oncogenic pathways provides a model for the study of other human cancer-associated mutations and can be used to complement and help decipher recent and impending whole cancer genome sequencing studies.

Methods

Primers/Oligonucleotides

For all sequences see Supplementary table 9

Transient transfections—Amino-terminal GFP-NPM1/GFP-Npm1 fusion constructs were generated and K562 cells photographed 24hrs after electroporation.

Npm1$^{flox\text{-}cA/+}$ ES cells and mice

A 9.8kb was retrieved from BAC bMQ-282D14 using oligonucleotide recombineering[29] and modified to the *Npm1$^{flox\text{-}cA}$* targeting construct (duplicated region: NCBIM37-chr11:33051153-33053141). *Npm1^{cA}* (Post-Cre) ES cell clones were derived under FIAU selection[30]. *Npm1$^{flox\text{-}cA/+}$* and *Npm1$^{flox\text{-}cA/flox\text{-}cA}$* mice were crossed with Stella-Cre for embryonic viability and *Mx1-Cre*[31] mice for hemopoietic studies. For *Mx1-Cre* activation 500μg pIpC x6 was used.

Stella-Cre mice

Generated by WW and PL by insertion of *IRES-Cre* into the 3'UTR of *Stella*, they show 100% Cre-*lox*P recombination at several loci in embryos and germline.

GrOnc mice

Generated by pronuclear injection of linearized *GrOnc* DNA.

Rosa$^{flox\text{-}SB}$ transposase mice

Generated as per Supplementary Figure 6.

Mouse genotyping

We used PCR assays with primers P1-P16 (e.g. Supplementary Figures 2, 6, 7).

Flow Cytometry & Cell Sorting

Mouse femurs and spleens were processed as described[32]. For BM lineage analysis we stained with Gr1-PE and CD11b(Mac1)-FITC, or B220-APC-Alexa750 and CD19-PE. For HSC/progenitor analyses, we depleted lineage-positive cells using MACS columns and stained with cKit-APC, ScaI-PB, CD34-FITC and either Flt3-PE (HSC) or FcRIII-PE (progenitors). Antibodies from BD Pharmingen except CD11b-FITC (Caltag). We used a CyAn-ADP analyzer and FlowJo. B220+ and Gr1+/Mac1+ cells were sorted using a MoFlo sorter. For leukemia phenotyping we used combinations of the above.

Gene expression profiling

Global profiling was done using Illumina mouse-6 expression beadchip version 2. Data were quantile normalised[33] and analyzed using the bioconductor (http://www.bioconductor.org/),

lumi (http://www.bioconductor.org/packages/2.0/bioc/html/lumi.html) and limma[34] packages, then p-value adjusted for multiple testing[35]. Microarray data and description of experimental design were deposited to Array Express with accession number E-MEXP-3113.

Hemopoietic colonies

BM or spleen cells were plated in M3434 (Stem Cell Technologies) as described[33]. Colonies were counted/picked after 10-12 days. For re-plating assays 50,000 BM cells from 6xNpm1$^{cA/+}$ and 6xNpm1^{WT} mice were plated and counted after 8 days with 30,000 cells re-plated etc.

Southern Blots

Npm1 targeting: *Pst*I-digested ES cell DNA was hybridized with a PCR-generated-probe (Figure 1b). *GrOnc* copy number and clonal integrations: *Sac*I-digested tail DNA or *Bam*HI-digested leukemic DNA respectively, were hybridized with the *Xba*I-*Sac*II *GrOnc* fragment (Supplementary Figure 5).

RT-PCR

For *Npm1*$^{+}$ and *Npm1*^{cA} cDNAs we used allele-specific primers R1-R3 and for *GrOnc-Csf2* primers Graffi1.4-LTR_F and Csf2_exon3_R.

qPCR/qRT-PCR

For *GrOnc* copy number *En2-SA* and *β-Actin* were quantified from tail DNA. *En2-SA*/*β-Actin* ratio was normalized against wild-type mice (2 copies of *En2-SA*). For *Csf2* qRT-PCR we designed specific primers/probe and normalized against *Gapdh*. For *Hox* genes, we used standardized assays (Applied Biosystems), normalized against Gapdh and expressed values relative to *Npm1*$^{+/+}$.

Anti-Npm1^{cA} specific antisera and Western Blots

Anti-Npm1^{cA}-specific rabbit antisera, were generated and affinity-purified using peptide Hydrazine-IQDLCLAVEEVSLRK and used at 1/100. Mouse monoclonal anti-Actin (Sigma) was used at 1/5000.

FISH analysis

The location of the 80-copy *GrOnc* donor site, was identified using Texas Red-labeled GrOnc DNA on blood metaphases.

Hematological measurements

Blood counts were performed on a VetABC analyzer (Horiba ABX).

Splinkerette PCR and sequencing

These were done as described[36] using *SB*-specific primers and 454-sequenced.

Identification of common integration sites (CISs)

ssaha2 was used to map *GrOnc* insertions to mouse genome. Sequences were filtered to contain the SBcommon-Sp2-454R primer then the end of the SB repeat, followed by genomic sequence starting with TA and ending at GATC (*Mbo*I restriction site). Sequences <17 nucleotides or with <85% maximal genomic identity were discarded. For sequences matching several loci, we calculated a normalized score difference (NSD) comparing the best hit to the second best hit, whereby NSD= ((score of best hit) − (score of second-best

hit)) / query-length*100. We mapped 5000 random mouse genomic fragments to the genome and found that 96.5% of correctly and only 1.5% of wrongly mapped reads had NSD ≥4 and removed reads with NSD <4 from analysis. Finally, redundant sequences from the same tumor and same location were "collapsed" to one integration. To identify CISs, non-redundant insertions were analyzed using a Gaussian Kernel Convolution-based framework[37] for 10Kb, 30Kb, 60Kb and 120Kb windows and all windows merged to compile CIS lists[38]. To identify previously described CISs we searched the retroviral tagged cancer gene database (RTCGD, http://rtcgd.ncifcrf.gov)[36] and recent insertional mutagenesis publications[3-4,39-40].

Histopathology

Formalin-fixed, paraffin-embedded sections were stained with H&E and anti-CD3, anti-B220 and anti-myeloperoxidase, detected by immunoperoxidase. All material was examined by two experienced histopathologists (PW and MA) blinded to mouse genotypes. A primary diagnosis was established and hemopoietic tissues examined for additional malignancies.

Gm-csf ELISA

Cryopreserved AML cells were plated in duplicate at 100,000 per 100ul RPMI/ 10%FCS. Supernatants were collected after 2 days and assayed (EMGMCSF, Thermo).

Leukemia Transplants

Syngeneic mice were sublethally irradiated (500rad) and injected with 1×10^6 cryopreserved AML cells into the tail vein. Mice were culled when unwell or after 180 days.

Statistics

We used Fisher's exact test for 2×2 comparisons and mutual exclusivity testing, χ^2-test for nominal data and t-test for continuous data unless normality test failed, when Mann-Whitney Rank Sum tests were used (Sigma Stat). SEMs are represented in error bars.

Supplementary Material

Refer to Web version on PubMed Central for supplementary material.

Acknowledgments

We acknowledge the use of the Research Support Facility at the WTSI, the Department of Pathology Tissue Bank and the Cambridge NIHR Biomedical Research Centre, University of Cambridge. We thank F. Law and J. Gadiot for assistance in generating the $Npm1^{flox\text{-}CA}$ and $Rosa^{flox\text{-}SB}$ mice, F. Foyer and B. Graham for help with fluorescent microscopy, B. Ling, W. Cheng, R. Macintyre and P. Chan for help with Flow Cytometry; R. Bautista for help with gene expression images; C, Hale and A. Nyzhnyk for help with ELISAs, B. Huntly, D. Adams, J. Cadinanos, H. Prosser, N. Conte, K. Yusa and Q. Liang, for helpful discussions during the project; P. Campbell and A. Green for critical reading of the manuscript. This work was supported by a Clinician Scientist Fellowship from Cancer Research UK (G.V.).

References

1. Falini B, et al. Cytoplasmic nucleophosmin in acute myelogenous leukemia with a normal karyotype. N Engl J Med. 2005; 352:254–266. [PubMed: 15659725]
2. Alcalay M, et al. Acute myeloid leukemia bearing cytoplasmic nucleophosmin (NPMc+ AML) shows a distinct gene expression profile characterized by up-regulation of genes involved in stem-cell maintenance. Blood. 2005; 106:899–902. doi:2005-02-0560 [pii] 10.1182/blood-2005-02-0560. [PubMed: 15831697]

3. Dupuy AJ, Akagi K, Largaespada DA, Copeland NG, Jenkins NA. Mammalian mutagenesis using a highly mobile somatic Sleeping Beauty transposon system. Nature. 2005; 436:221–226. [PubMed: 16015321]
4. Collier LS, Carlson CM, Ravimohan S, Dupuy AJ, Largaespada DA. Cancer gene discovery in solid tumours using transposon-based somatic mutagenesis in the mouse. Nature. 2005; 436:272–276. doi:nature03681 [pii] 10.1038/nature03681. [PubMed: 16015333]
5. Okuwaki M. The structure and functions of NPM1/Nucleophsmin/B23, a multifunctional nucleolar acidic protein. J Biochem. 2008; 143:441–448. doi:mvm222 [pii] 10.1093/jb/mvm222. [PubMed: 18024471]
6. Grisendi S, Mecucci C, Falini B, Pandolfi PP. Nucleophosmin and cancer. Nat Rev Cancer. 2006; 6:493–505. doi:nrc1885 [pii] 10.1038/nrc1885. [PubMed: 16794633]
7. Hingorani K, Szebeni A, Olson MO. Mapping the functional domains of nucleolar protein B23. J Biol Chem. 2000; 275:24451–24457. doi:10.1074/jbc.M003278200 M003278200 [pii]. [PubMed: 10829026]
8. Falini B, et al. Altered nucleophosmin transport in acute myeloid leukaemia with mutated NPM1: molecular basis and clinical implications. Leukemia. 2009; 23:1731–1743. doi:leu2009124 [pii] 10.1038/leu.2009.124. [PubMed: 19516275]
9. Falini B, et al. NPM1 mutations and cytoplasmic nucleophosmin are mutually exclusive of recurrent genetic abnormalities: a comparative analysis of 2562 patients with acute myeloid leukemia. Haematologica. 2008; 93:439–442. doi:haematol.12153 [pii] 10.3324/haematol.12153. [PubMed: 18268276]
10. Rocquain J, et al. Combined mutations of ASXL1, CBL, FLT3, IDH1, IDH2, JAK2, KRAS, NPM1, NRAS, RUNX1, TET2 and WT1 genes in myelodysplastic syndromes and acute myeloid leukemias. BMC Cancer. 2010; 10:401. doi:1471-2407-10-401 [pii] 10.1186/1471-2407-10-401. [PubMed: 20678218]
11. Cheng K, et al. The cytoplasmic NPM mutant induces myeloproliferation in a transgenic mouse model. Blood. 2010; 115:3341–3345. doi:blood-2009-03-208587 [pii] 10.1182/blood-2009-03-208587. [PubMed: 19666870]
12. Sportoletti P, et al. Npm1 is a haploinsufficient suppressor of myeloid and lymphoid malignancies in the mouse. Blood. 2008; 111:3859–3862. doi:blood-2007-06-098251 [pii] 10.1182/blood-2007-06-098251. [PubMed: 18212245]
13. Lavau C, Szilvassy SJ, Slany R, Cleary ML. Immortalization and leukemic transformation of a myelomonocytic precursor by retrovirally transduced HRX-ENL. EMBO J. 1997; 16:4226–4237. [PubMed: 9250666]
14. Kogan SC, et al. Bethesda proposals for classification of nonlymphoid hematopoietic neoplasms in mice. Blood. 2002; 100:238–245. [PubMed: 12070033]
15. Smith GS, Walford RL, Mickey MR. Lifespan and incidence of cancer and other diseases in selected long-lived inbred mice and their F 1 hybrids. J Natl Cancer Inst. 1973; 50:1195–1213. [PubMed: 4351393]
16. Rad R, et al. PiggyBac Transposon Mutagenesis: A Tool for Cancer Gene Discovery in Mice. Science. 2010; 330:1104–1107. doi:science.1193004 [pii] 10.1126/science.1193004. [PubMed: 20947725]
17. Voisin V, Barat C, Hoang T, Rassart E. Novel insights into the pathogenesis of the Graffi murine leukemia retrovirus. J Virol. 2006; 80:4026–4037. [PubMed: 16571819]
18. de Ridder J, Uren A, Kool J, Reinders M, Wessels L. Detecting statistically significant common insertion sites in retroviral insertional mutagenesis screens. PLoS Comput Biol. 2006; 2:e166. doi: 06-PLCB-RA-0052R3 [pii] 10.1371/journal.pcbi.0020166. [PubMed: 17154714]
19. Duhrsen U, Stahl J, Gough NM. In vivo transformation of factor-dependent hemopoietic cells: role of intracisternal A-particle transposition for growth factor gene activation. EMBO J. 1990; 9:1087–1096. [PubMed: 2108861]
20. Rogers SY, Bradbury D, Kozlowski R, Russell NH. Evidence for internal autocrine regulation of growth in acute myeloblastic leukemia cells. Exp Hematol. 1994; 22:593–598. [PubMed: 7516889]

21. Young DC, Griffin JD. Autocrine secretion of GM-CSF in acute myeloblastic leukemia. Blood. 1986; 68:1178–1181. [PubMed: 3490289]
22. Takeda A, Sarma NJ, Abdul-Nabi AM, Yaseen NR. Inhibition of CRM1-mediated nuclear export of transcription factors by leukemogenic NUP98 fusion proteins. J Biol Chem. 2010; 285:16248–16257. doi:M109.048785 [pii] 10.1074/jbc.M109.048785. [PubMed: 20233715]
23. Kim R, et al. Genome-based identification of cancer genes by proviral tagging in mouse retrovirus-induced T-cell lymphomas. J Virol. 2003; 77:2056–2062. [PubMed: 12525640]
24. Lauchle JO, et al. Response and resistance to MEK inhibition in leukaemias initiated by hyperactive Ras. Nature. 2009; 461:411–414. doi:nature08279 [pii] 10.1038/nature08279. [PubMed: 19727076]
25. Nakamura T, Largaespada DA, Shaughnessy JD Jr. Jenkins NA, Copeland NG. Cooperative activation of Hoxa and Pbx1-related genes in murine myeloid leukaemias. Nat Genet. 1996; 12:149–153. doi:10.1038/ng0296-149. [PubMed: 8563752]
26. Ayton PM, Cleary ML. Transformation of myeloid progenitors by MLL oncoproteins is dependent on Hoxa7 and Hoxa9. Genes Dev. 2003; 17:2298–2307. doi:10.1101/gad.1111603 1111603 [pii]. [PubMed: 12952893]
27. Lawrence HJ, et al. Mice bearing a targeted interruption of the homeobox gene HOXA9 have defects in myeloid, erythroid, and lymphoid hematopoiesis. Blood. 1997; 89:1922–1930. [PubMed: 9058712]
28. Ley TJ, et al. DNMT3A Mutations in Acute Myeloid Leukemia. N Engl J Med. 2010 doi:10.1056/NEJMoa1005143.
29. Liu P, Jenkins NA, Copeland NG. A highly efficient recombineering-based method for generating conditional knockout mutations. Genome Res. 2003; 13:476–484. doi:10.1101/gr.749203. [PubMed: 12618378]
30. Chen YT, Bradley A. A new positive/negative selectable marker, puDeltatk, for use in embryonic stem cells. Genesis. 2000; 28:31–35. doi:10.1002/1526-968X(200009)28:1<31::AID-GENE40>3.0.CO;2-K [pii]. [PubMed: 11020714]
31. Kuhn R, Schwenk F, Aguet M, Rajewsky K. Inducible gene targeting in mice. Science. 1995; 269:1427–1429. [PubMed: 7660125]
32. Li J, et al. JAK2 V617F impairs hematopoietic stem cell function in a conditional knock-in mouse model of JAK2 V617F-positive essential thrombocythemia. Blood. 2010; 116:1528–1538. [PubMed: 20489053]
33. Yang YH, et al. Normalization for cDNA microarray data: a robust composite method addressing single and multiple slide systematic variation. Nucleic Acids Res. 2002; 30:e15. [PubMed: 11842121]
34. Smyth GK. Linear models and empirical bayes methods for assessing differential expression in microarray experiments. Stat Appl Genet Mol Biol. 2004; 3 Article3, doi: 10.2202/1544-6115.1027.
35. Benjamini Y, Hochberg Y. Controlling the false discovery rate: A practical and powerful approach to multiple testing. J Roy Stat Soc, Ser B. 1995; 57:289–300.
36. Uren AG, et al. A high-throughput splinkerette-PCR method for the isolation and sequencing of retroviral insertion sites. Nat Protoc. 2009; 4:789–798. doi:nprot.2009.64 [pii] 10.1038/nprot.2009.64. [PubMed: 19528954]
37. de Ridder J, Uren A, Kool J, Reinders M, Wessels L. Detecting statistically significant common insertion sites in retroviral insertional mutagenesis screens. PLoS Comput Biol. 2006; 2:e166. doi: 06-PLCB-RA-0052R3 [pii] 10.1371/journal.pcbi.0020166. [PubMed: 17154714]
38. Akagi K, Suzuki T, Stephens RM, Jenkins NA, Copeland NG. RTCGD: retroviral tagged cancer gene database. Nucleic Acids Res. 2004; 32:D523–527. doi:10.1093/nar/gkh013 32/suppl_1/D523 [pii]. [PubMed: 14681473]
39. Collier LS, et al. Whole-body sleeping beauty mutagenesis can cause penetrant leukemia/lymphoma and rare high-grade glioma without associated embryonic lethality. Cancer Res. 2009; 69:8429–8437. doi:0008-5472.CAN-09-1760 [pii] 10.1158/0008-5472.CAN-09-1760. [PubMed: 19843846]

40. Uren AG, et al. Large-scale mutagenesis in p19(ARF)- and p53-deficient mice identifies cancer genes and their collaborative networks. Cell. 2008; 133:727–741. doi:S0092-8674(08)00436-4 [pii] 10.1016/j.cell.2008.03.021. [PubMed: 18485879]

Europe PMC Funders Author Manuscripts

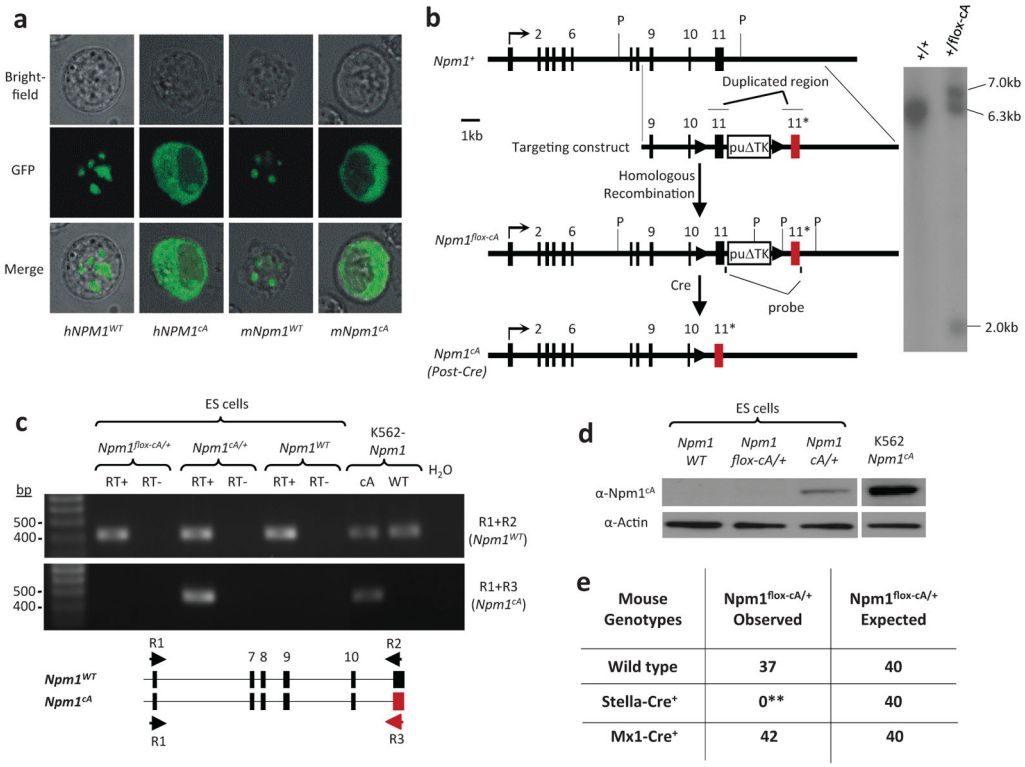

Mouse Genotypes	Npm1flox-cA/+ Observed	Npm1flox-cA/+ Expected
Wild type	37	40
Stella-Cre+	0**	40
Mx1-Cre+	42	40

Figure 1. Conditional mouse model of type A *NPM1c* mutation

a, N-terminal GFP-fusions of type A human *(NPM1^{cA})* and "humanized" mouse (*Npm1^{cA}*) mutants show identical sub-cellular distribution. **b,** The conditional *Npm1$^{flox\text{-}cA}$* allele interferes minimally with the native locus and converts to mutant *Npm1^{cA}* allele by Cre (humanized mutant exon 11* in red; mouse exon 11 is homologous to human exon 12). **c-d,** *Npm1^{cA}* RNA and protein detected in Post-Cre ES cells by RT-PCR (c) and Western Blot (d) respectively. **e,** Universal lethality of *Npm1$^{flox\text{-}cA/+}$; Stella-Cre^{+}* (** p=0.0001) versus mendelian ratios for *Npm1$^{flox\text{-}cA/+}$; Mx1-Cre^{+}* mice.

P, *Pst*I site; PuΔTK, Puro-Delta-TK cassette; K562-Npm1, K562 cells transfected with *Npm1^{cA}* or *Npm1^{WT}* cDNA; RT, Reverse Transcriptase, RT-PCR primers: R1, forward; R2, *Npm1^{WT}* reverse; R3, *Npm1^{cA}* reverse (red).

Europe PMC Funders Author Manuscripts

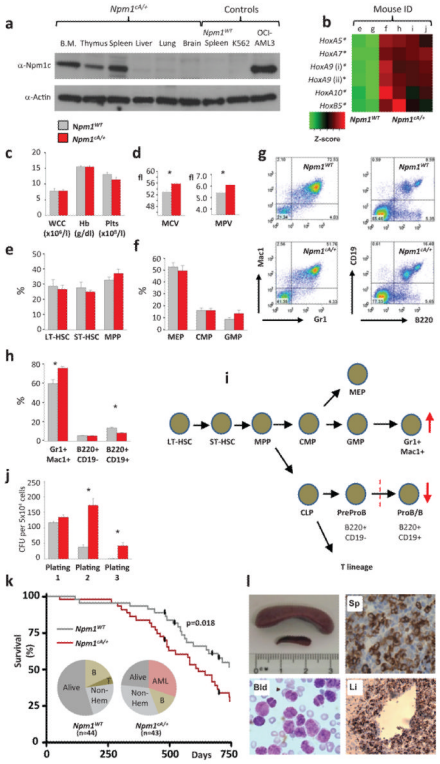

Figure 2. Hematopoietic changes and incidence of AML in *Npm1*$^{cA/+}$ mice

a, Hemopoietic expression of Npm1^{cA} protein in *Npm1*$^{cA/+}$ mice. **b,** *Hox*-overexpression in *Npm1*$^{cA/+}$ vs *Npm1*^{WT} lineage negative hemopoietic progenitors. **c,d,** No significant differences in white cell (WCC), hemoglobin (Hb) or platelet counts (Plts), but higher mean red cell (MCV) and platelet (MPV) volumes in *Npm1*$^{cA/+}$ mice. **e,f,** No differences in marrow stem and progenitor cell compartment sizes. **g,h,** Expansion of mature myeloid (Gr1^{+}/Mac1^{+}) and reduction in late (B220^{+}/CD19^{+}) B-cells in *Npm1*$^{cA/+}$ vs *Npm1*^{WT} marrow. **i,** Summary of hemopoietic changes in Npm1$^{cA/+}$ mice. **j,** Increased serial re-plating of Npm1$^{cA/+}$ myeloid progenitors. **k,** Decreased survival of *Npm1*$^{cA/+}$ mice due to excess AML. **l,** Example of AML showing splenomegaly due to infiltration with myeloperoxidase-positive blasts (Sp), also infiltrating the liver (Li) and blood (Bld).

Error bars show the standard error of the mean; *p<0.05; B,T, B or T-cell leukemia/ lymphoma; Non-Hem, Non-hematological.

Europe PMC Funders Author Manuscripts

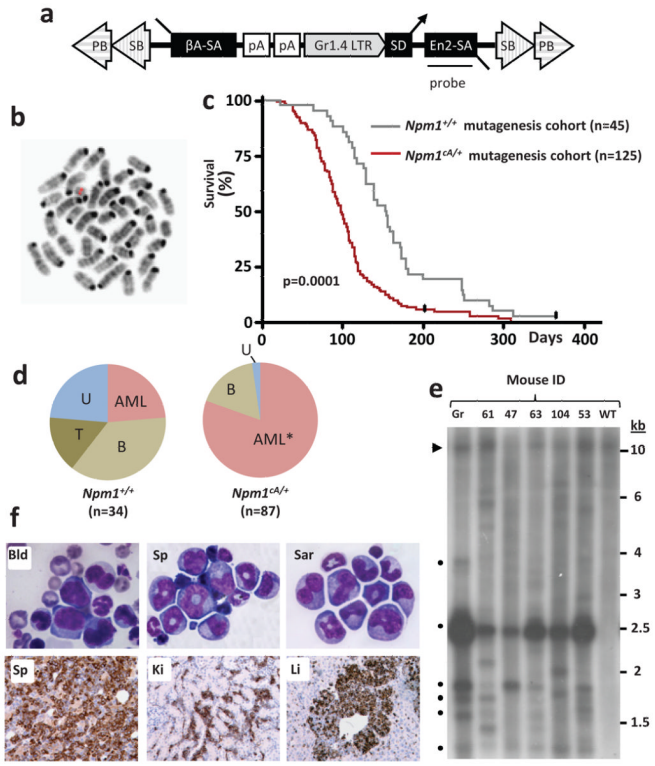

Figure 3. *Npm1*^{cA} and the *GrOnc* transposon synergize to cause AML

a, The *GrOnc* transposon carrying gene-activating and inactivating elements flanked by repeats for the *Sleeping Beauty* (SB) and *PiggyBac* (PB). **b,** Blood-metaphase FISH showing the genomic location of the GrOnc donor locus on chromosome 19. **c,** Acceleration of leukemogenesis in *Npm1*$^{cA/+}$ compared to *Npm1*$^{+/+}$ mutagenised mice. **d,** Marked increase in the proportion of AMLs and absence of T cell tumors in *Npm1*$^{cA/+}$ compared to *Npm1*$^{+/+}$ mice. **e,** Southern blot showing clonal transposon integrations in mouse leukemias. Endogenous *En2* (arrowhead) and GrOnc donor locus concatamer (dots) bands indicated. **f,** Morphology and immunohistochemistry (anti-myeloperoxidase) from an *Npm1*$^{cA/+}$ AML. *Gr1.4 LTR*, Graffi1.4 MuLV long terminal repeat; *SD*, Lun splice donor; *En2-SA and βA-SA*, *Engrailed 2* and *Carp β-actin* splice acceptor; *pA*, adenovirus polyadenylation signal; *p<0.00001; B, T and U, B-cell, T-cell and undifferentiated leukemia/lymphoma; Bld, blood; Sp, spleen; Sar, myeloid sarcoma; Ki, kidney; Li, liver.

Europe PMC Funders Author Manuscripts

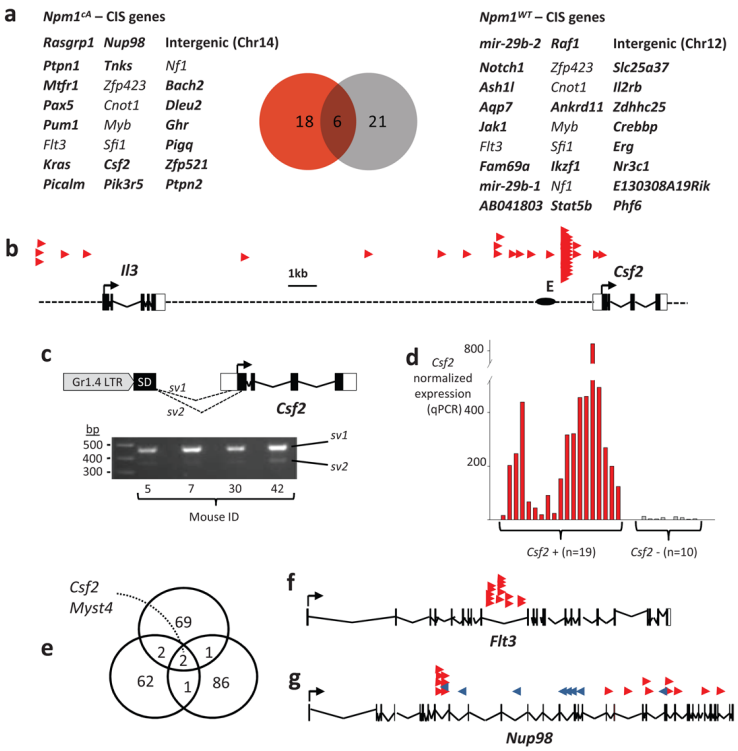

Figure 4. Common integration sites in transposon-derived leukemias

a, Common integration sites in Npm1$^{cA/+}$ and Npm1$^{+/+}$mice show some overlap (regular font) but are mostly different (bold). **b-d,** Directional *GrOnc* integrations at the *Csf2* locus identified in 42 of 70 AMLs, were associated with the formation of two *LunSD-Csf2* fusion mRNA splice variants (sv1 and sv2) and marked overexpression of *Csf2* mRNA (note break in Y axis). **e,** *GrOnc* integrations in three individual myeloid blast colonies from one of these AMLs shared only 2 insertions, involving *Csf2* and the myeloid oncogene *Myst4(Moz)* suggesting that these were “driver” insertions. **e,** Directional activating integrations in intron 9 of *Flt3*. **g,** Bi-directional integrations in *Nup98*.

Europe PMC Funders Author Manuscripts

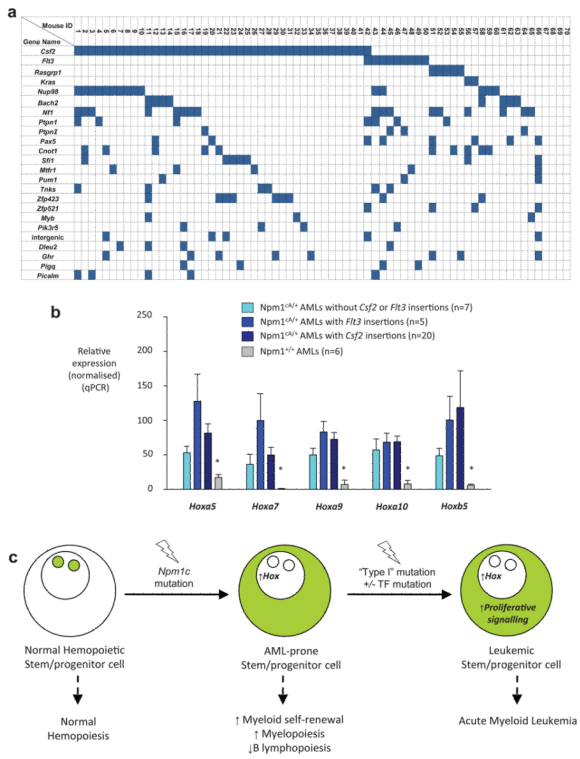

Figure 5. A model for Npm1$^{cA/+}$-driven leukemogenesis

a, Co-occurrence table of CIS genes in 70 NPm1$^{cA/+}$ AMLs reveals mutually exclusive insertions in *Csf2*, *Flt3*, *Rasgrp1* and *Kras*. **b,** Persistence of *Hox* overexpression in *Npm1*$^{cA/+}$ vs *Npm1*$^{+/+}$ AMLs indicating that this effect of Npm1cA persists in leukemic cells(* p≤0.03). **c.** Model for Npm1^{cA} - driven leukemogenesis supported by our data: isolated *Npm1*^{cA} increases self renewal but leukemic transformation only occurs upon activation of defined proliferative pathways (Type I mutation), facilitated by a permissive transcription factor (TF) mutation.

Error bars show the standard error of the mean. Localization of Npm1 protein indicated in green.

Europe PMC Funders Author Manuscripts